Molecular Biology of the Cell
Vol. 20, 1374–1387, March 1, 2009

Essential Role of hIST1 in Cytokinesis

Monica Agromayor,* Jez G. Carlton,* John P. Phelan,† Daniel R. Matthews,‡ Leo M. Carlin,‡ Simon Ameer-Beg,‡ Katherine Bowers,† and Juan Martin-Serrano*

*Department of Infectious Diseases, King's College London School of Medicine, London SE1 9RT, United Kingdom; ‡The Richard Dimbleby Department of Cancer Research and The Randall Division of Cell and Molecular Biophysics, King's College London School of Medicine, London SE1 9RT, United Kingdom; and †Institute of Structural and Molecular Biology, Division of Biosciences, University College London, London WC1E 6BT, United Kingdom

Submitted May 13, 2008; Revised November 13, 2008; Accepted December 23, 2008
Monitoring Editor: Stephen Doxsey

The last steps of multivesicular body (MVB) formation, human immunodeficiency virus (HIV)-1 budding and cytokinesis require a functional endosomal sorting complex required for transport (ESCRT) machinery to facilitate topologically equivalent membrane fission events. Increased sodium tolerance (*IST*) *1*, a new positive modulator of the ESCRT pathway, has been described recently, but an essential function of this highly conserved protein has not been identified. Here, we describe the previously uncharacterized KIAA0174 as the human homologue of *IST1* (hIST1), and we report its conserved interaction with VPS4, CHMP1A/B, and LIP5. We also identify a microtubule interacting and transport (MIT) domain interacting motif (MIM) in hIST1 that is necessary for its interaction with VPS4, LIP5 and other MIT domain-containing proteins, namely, MITD1, AMSH, UBPY, and Spastin. Importantly, hIST1 is essential for cytokinesis in mammalian cells but not for HIV-1 budding, thus providing a novel mechanism of functional diversification of the ESCRT machinery. Last, we show that the hIST1 MIM activity is essential for cytokinesis, suggesting possible mechanisms to explain the role of hIST1 in the last step of mammalian cell division.

INTRODUCTION

Multivesicular bodies (MVBs) are endocytic organelles characterized by their ability to bud away from the cytosol to generate intraluminal vesicles (ILVs). The MVB is a major protein sorting station in the cell, in which specific membrane proteins are sorted into the ILVs, whereas others remain on the limiting membrane. The endosomal sorting complex required for transport (ESCRT) machinery mediates sorting of ubiquitinated cargo proteins into the forming ILVs (Gruenberg and Stenmark, 2004; Hurley and Emr, 2006). These sorting and vesicle formation events require the sequential assembly of ESCRT-I, -II, and -III on the endosomal membranes, and the whole process is regulated by the essential activity of VPS4, an AAA-ATPase that mediates the disassembly of the ESCRT complexes for recycling purposes (Babst *et al*., 1998; Katzmann *et al*., 2001; Babst *et al*., 2002a,b). Thus, spatial and temporal regulation of VPS4 seems essential for the function of the ESCRT machinery. In fact, a conserved mechanism of VPS4 regulation by Vta1/LIP5 has been described, showing that a dimeric form of Vta1 stimulates the ATPase activity of Vps4 by promoting its multimerization into a catalytically active double hexameric ring that pulls the ESCRT complexes into the central channel of the lower ring, releasing the disassembled subunits into the cytoplasm (Azmi *et al*., 2006, 2008; Xiao *et al*., 2008).

This article was published online ahead of print in *MBC in Press* (http://www.molbiolcell.org/cgi/doi/10.1091/mbc.E08–05–0474) on January 7, 2009.

Address correspondence to: Juan Martin-Serrano (juan.martin_serrano@kcl.ac.uk).

ESCRT-III seems to be the core machinery that mediates the membrane deformation and fission events required for ILV formation during sorting of the ubiquitinated cargo into the MVB (Hurley and Emr, 2006; Hanson *et al*., 2008). After completion of the process, VPS4 is recruited by ESCRT-III through the direct interaction of the MIT domain in VPS4 with a conserved MIT-interacting motif (MIM) present at the C-terminal region of some of the ESCRT-III subunits (Obita *et al*., 2007; Stuchell-Brereton *et al*., 2007). In addition to binding VPS4, these MIMs coordinate the interaction of ESCRT-III with other activities encoded by MIT domain-containing proteins, such as deubiquitinating enzymes (Agromayor and Martin-Serrano, 2006; McCullough *et al*., 2006; Tsang *et al*., 2006; Row *et al*., 2007). A further regulatory mechanism in the pathway is provided by Vps46/CHMP1A,-1B, a peripherally associated ESCRT-III protein that regulates the interaction of VPS4 with endosomal membranes (Lottridge *et al*., 2006; Nickerson *et al*., 2006).

Many enveloped viruses, including human pathogens such as HIV-1 and Ebola virus, recruit the ESCRT machinery to facilitate the final steps of infectious viral particle formation (reviewed in Demirov and Freed, 2004; Morita and Sundquist, 2004; Bieniasz, 2006), a process that requires a membrane fission event that is topologically identical to MVB formation. An understanding of the MVB protein sorting machinery has provided essential clues to unmasking the cellular machinery recruited by different short amino acid sequences called late budding domains (L-domains). It is now established that many enveloped viruses encode four known types of L-domains (PT/SAP, PPXY, LYPXL, or FPIV motifs), which use ESCRT-III via the direct interaction with adaptor proteins such as TSG101 (PTAP motif) (Garrus *et al*., 2001; Martin-Serrano *et al*., 2001; VerPlank *et al*., 2001; Demirov *et al*., 2002), ALIX (LYPxL motif) (Martin-Serrano *et*

al., 2003; Strack *et al*., 2003; von Schwedler *et al*., 2003), or HECT ubiquitin ligases (PPXY motif) (Freed, 2002; Martin-Serrano, 2007) and unknown adaptor (FPIV) (Schmitt *et al*., 2005). One emerging theme is the possibility that, in addition to these adaptor proteins, L-domain activity requires only the ESCRT proteins that are involved in membrane fission, as suggested by the fact that ESCRT-II, CHMP6, or AMSH are dispensable for HIV-1 egress (Agromayor and Martin-Serrano, 2006; Langelier *et al*., 2006).

Recent work has identified a functional requirement for the ESCRT complexes during the last step of cell division, another membrane scission event that is topologically similar to MVB formation and retroviral budding (Carlton and Martin-Serrano, 2007; Morita *et al*., 2007; Carlton *et al*., 2008). Completion of cytokinesis requires abscission of the midbody, a microtubule-rich cytoplasmic bridge that connects the daughter cells preceding their separation (Glotzer, 2001; Barr and Gruneberg, 2007). Many proteins required for abscission localize at the Flemming body, a protein-dense structure at the central region of the midbody that also contains interdigitating microtubules (Eggert *et al*., 2006). Importantly, the ESCRT components TSG101 and ALIX are recruited to the Flemming body via the interaction with CEP55, a midbody component required for abscission (Carlton and Martin-Serrano, 2007; Morita *et al*., 2007; Carlton *et al*., 2008). Functional studies using small interfering RNA (siRNA) have shown that both Tsg101 and ALIX are required for midbody abscission, and a role for ESCRT-III is also suggested by the inhibition of cytokinesis in cells overexpressing yellow fluorescent protein (YFP)-CHMP4 or a catalytically inactive VPS4 (Carlton and Martin-Serrano, 2007; Morita *et al*., 2007; Carlton *et al*., 2008). More direct evidence supporting the essential role of ESCRT-III in abscission is provided by the cytokinetic defects in cells expressing an ALIX mutant that is specifically mutated in the CHMP4-binding surface (Morita *et al*., 2007; Carlton *et al*., 2008).

We have now identified human increased sodium tolerance (hIST)1 as an evolutionarily conserved component of the mammalian ESCRT machinery that binds to VPS4, LIP5, CHMP1A, and CHMP1B. In agreement with recent reports (Dimaano *et al*., 2008; Rue *et al*., 2008), we show that yeast Ist1 is not essential for endosomal sorting, although a synthetic interaction with Vta1 is observed, suggesting that Ist1 is a positive modulator of the class E vps pathway. We also demonstrate a specific requirement of hIST1 for cytokinesis in mammalian cells but not for HIV-1 budding, showing a novel mechanism of functional diversification in the ESCRT pathway. We show for the first time that the function of hIST1 in the last step of mammalian cell division requires a novel MIM capable of binding to a wide array of MIT-containing proteins.

MATERIALS AND METHODS

Plasmid Construction

hIST1 was amplified by polymerase chain reaction (PCR) from IMAGE clone 6502833 by using primers directed to the 5′ and 3′ ends of the coding sequence containing EcoRI and XhoI sites to insert the PCR product into pGBKT7 (Clontech, Mountain View, CA) and pVP16 (Bogerd *et al*., 1993) for yeast two-hybrid assays and into pCR3.1/YFP and pCAGGS/glutathione transferase (GST) for protein expression experiments. hIST1 deletions and point mutant derivatives were generated by PCR in a similar way. siRNA-resistant forms of hIST1 (hIST1^{R}) were created using PCR-based methodologies to introduce silent mutations in the sequence 179LIEIAKN185 and cloned as an N-terminal YFP fusion into pCMS28-YFP-EcoRI-NotI-XhoI, a bicistronic retroviral packaging vector encoding a puromycin resistance gene linked via an internal ribosomal entry site to the multiple cloning site. Similarly, tubulin was PCR amplified and cloned as an N-terminal mCherry fusion into pCMS28-mCherry-NotI. All the yeast two-hybrid plasmids and human class E VPS expression plasmids have been described previously (Martin-Serrano *et al*., 2003). pGEX CHMP1B 180-196 was a gift from W. Sundquist and was modified and used to generate pGEX hIST1 362-379 by inserting annealed oligonucleotides (oligos) containing the sequence for the last 17 amino acids of hIST1 with EcoRI and XhoI overhangs.

Yeast Strains and Media

Yeast strains used in this study are shown in Supplemental Table 1. Strains were constructed by standard genetic techniques and grown in rich medium (YEPD; Burke *et al*., 2000) or synthetic dextrose minimal medium with appropriate amino acid supplements (SD; Burke *et al*., 2000).

Yeast Growth and Carboxypeptidase Y (CPY) Secretion Assays

CPY secretion was monitored using a colony overlay assay as described previously (Roberts *et al*., 1991). For growth curves, yeast strains were inoculated into YEPD medium and monitored hourly at $OD_{600\ nm}$ in a spectrophotometer.

RNA Interference (RNAi)

siRNAs targeting either luciferase (CUGCCUGCGUGAGAUUCUC), TSG101 (CCUCCAGUCUUCUCUCGUC), ALIX (GAAGGAUGCUUUCGAUAAAUU), or CEP55 (GGAGAAGAAUGCUUAUCAA) are from Dharmacon RNA Technologies (Lafayette, CO). Additionally, siGENOME SMARTpool targeting hIST1 (hIST1-SP) was purchased from Dharmacon RNA Technologies (catalog no. M-020977-00) and two separate oligos matching selected regions of the hIST1 sequence (hIST-3: CTGATTGAAATTGCAAAGAAT and hIST-4: TCGCCTTAAACTATTGGAGAA) were purchased from QIAGEN (Hilden, Germany) (catalog nos. SI00452410 and SI00452417).

Generation of Stable Cell Lines

293T cells were transfected with 100 ng of pHIT-VSVG, 700 ng of MLV-GagPol, and 200 ng of the pCMS28-YFPhIST1^{R}, pCMS28-YFPhIST1^{R} L375A/K376A, or pCMS28-mCherryTubulin retroviral packaging vector for 48 h. 293T supernatants were collected and used to transduce HeLa cells. 48 h after transduction, selection with puromycin (200 ng/ml) was applied and cells were passaged under continual selection. Cells stably expressing ALIX, CEP55, and TSG101 have been described previously (Carlton and Martin-Serrano, 2007).

Yeast Two-Hybrid Assay

Yeast Y190 cells were transformed with 1 μg of each of the indicated pGBKT7 and pVP16 constructs, and transformants were selected on media lacking tryptophan and leucine for 3 d at 30°C. Interactions were determined by β-galactosidase activity in liquid yeast extracts using chlorophenol red-β-D-galactopyranoside (Roche Diagnostics, Mannheim, Germany) as a substrate.

Coprecipitation Assays

293T cells were transfected with GST and YFP expression vectors (1 μg of each) by using polyethylenimine (Polysciences, Warrington, PA) (Durocher *et al*., 2002). Thirty-six hours later, cells were harvested and lysed in 1 ml of 50 mM Tris-HCl, pH 7.4, 150 mM NaCl, 5 mM EDTA, 5% glycerol, 1% Triton X-100, and a protease inhibitor cocktail (complete mini-EDTA free; Roche Diagnostics). Clarified lysates were incubated with glutathione-Sepharose beads (GE Healthcare, Little Chalfont, Buckinghamshire, United Kingdom) for 3 h at 4°C and washed three times with wash buffer (50 mM Tris-HCl, pH 7.4, 150 mM NaCl, 5 mM EDTA, 5% glycerol, and 0.1% Triton X-100). The bead-bound proteins were eluted by boiling in 100 μl of SDS sample buffer and analyzed by Western blotting with α-green fluorescent protein (GFP) monoclonal antibody (mAb).

In CHMP1B and hIST1 MIMs, an extra step was added to the coprecipitation protocol as follows. BL21 bacteria were transformed with the indicated pGEX plasmid, and protein expression was induced with 0.5 mM isopropyl β-D-thiogalactoside. Three hours after induction, bacteria were harvested, resuspended in 1 ml of lysis buffer (50 mM Tris, pH 7.4, 50 mM NaCl, 5 mM β-mercaptoethanol, 0.2% deoxycholate, and 0.25 mg of lysozyme), and incubated at 4°C for 40 min. Soluble proteins were collected after centrifugation, and GST-beads were preincubated with 100 μl of the supernatant for 1 h at 4°C. Unbound proteins were removed by washing as described above, and 900 μl of the cell lysates from 293T cells transfected with the indicated YFP expression plasmids was added to the beads.

Epidermal Growth Factor (EGF) Receptor Degradation Assay

HeLa cells were transfected with 50 pmol of siRNA by using Dharmafect1 (Dharmacon RNA Technologies). The next day, cells were serum starved over night in DMEM containing 0.2% fatty acid-free bovine serum albumin (Sigma-Aldrich, St. Louis, MO). The next morning, cells were treated with 5 μg/ml cycloheximide (Sigma-Aldrich) for 1 h before stimulation with 50

ng/ml EGF (Sigma-Aldrich) for 0, 30, 90, or 180 min in the presence of cycloheximide. At the required time point, cells were harvested and resuspended in 100 μl of SDS sample buffer. Endogenous EGF receptor was analyzed by Western blotting with α-epidermal growth factor receptor (EGFR) antibody (Cell Signaling Technology, Beverly, MA) and Alexa-conjugated secondary antibodies obtained from Li-Cor Biosciences (Lincoln, NE). Membranes were imaged and quantified with the Odyssey imaging system (Li-Cor Biosciences).

Human Immunodeficiency Virus (HIV) Infectivity Assays

Cells were transfected with 500 ng of the YFP fusions and 300 ng of pNL/HXB. Indicator HeLa-TZM-bl cells ($CD4^+$, CXCR4+, CCR5+, and HIV-1 LTR-LacZ) (Derdeyn *et al*., 2000) were infected with 1 μl of supernatant, harvested from 293T cells 36 h after transfection. Finally, 48 h after infection, β-galactosidase activities in cell lysates were measured using the chemiluminescent detection reagent Galacto-Star (Applied Biosystems, Foster City, CA). Culture supernatants, collected 48 h after transfection, were clarified by low-speed centrifugation, and particles present in 250 μl were obtained by centrifugation through a 20% sucrose cushion at 14,000 rpm for 2 h. Viral protein content in cell and particle lysates was analyzed by Western blotting with α-Gag antibody.

To assay inhibition of viral production by siRNA-mediated depletion of cellular hIST1, 293T cells were initially transfected with 50 pmol of siRNA by using Dharmafect1 (Dharmacon RNA Technologies) and split the next day. Forty-eight hours after initial transfection, cells were cotransfected with another 50 pmol of siRNA and the HIV proviral plasmid using Lipofectamine 2000 (Invitrogen, Carlsbad, CA).

Multinucleation Assays

HeLa cells (25,000) were seeded in a 48-well plate and 2 h after plating were transfected with 50 pmol of siRNA targeting either luciferase, CEP55, ALIX, or hIST1 by using Dharmafect-1 (Dharmacon RNA Technologies). Forty-eight hours later, cells were reseeded onto glass coverslips and transfected again with 50 pmol of siRNA for another 48 h. Cells were then fixed and identified through α-tubulin staining. Three hundred cells per coverslip were scored for the presence of more than one nucleus. Cells unambiguously connected by midbodies were considered multinucleated.

For RNAi rescue assays, stable HeLa cell lines expressing YFP-siRNA–resistant hIST1 or YFP-siRNA–resistant hIST1 L375A/K376A were treated with the indicated siRNA, fixed, stained with α-tubulin, and scored for multinucleation or arrest at midbody stage as described above.

Imaging

For overexpression assays, HeLa cells were seeded onto glass coverslips and transfected with YFP-VPS4 E228Q expression plasmid. Cells were fixed with 4% paraformaldehyde 24 h after transfection, mounted in Mowiol, and images were taken using an AOBS SP2 confocal microscope (Leica, Wetzlar, Germany).

For multinucleation assays, cells were treated with siRNA as described above, fixed with 3% paraformaldehyde for 15 min, permeabilized with phosphate-buffered saline (PBS), 0.1% Triton X-100 for 5 min, and then stained with monoclonal α-tubulin (DM1a) (Sigma-Aldrich) in PBS, 1% bovine serum albumin for 2 h. Alexa594-conjugated secondary antibody was applied in PBS for 1 h. Nuclei were visualized using Hoechst 33258, and coverslips were mounted in Mowiol. Similarly, for analysis of endogenous hIST1 protein, HeLa cells were seeded onto glass coverslips and double stained with rabbit polyclonal α-hIST1 (gift from W. Sundquist, University of Utah, Salt Lake City, UT) and one of the following monoclonal antibodies: α-tubulin, α-EEA1 (BD Biosciences, San Jose, CA), α-Snx1 (BD Biosciences), α-CD63, α-lysosomal membrane protein (Lamp)1 or α-Lamp2 (Developmental Studies Hybridoma Bank, University of Iowa, Iowa City, IA) followed by staining with Alexa594- and 488-conjugated antibodies.

HeLa cells stably expressing YFP-CEP55, mCherry-ALIX, mCherry-TSG101, and mCherry-tubulin were treated with luciferase or hIST1 siRNAi, seeded onto glass coverslips, and stained with antibodies against α-tubulin, MKLP1 (N-19; Santa Cruz Biotechnology, Santa Cruz, CA), or AuroraB (AIM-1; BD Biosciences).

Time-Lapse Microscopy

siRNA-transfected HeLa cells stably expressing mCherry-tubulin were observed using a custom-built automated microscope developed at the Randall Division, King's College London, United Kingdom, for high-content screening microscopy. The time-lapse microscopy element of the instrument is equipped with a fiber coupled lamp (Nikon, Tokyo, Japan), a motorized stage (Märzhauser, Wetzlar, Germany), a closed-loop objective positioning mount (Piezo-Jena, Jena, Germany), with a 300-μm range of travel, and a motorized filter cube selector. All of these components are controlled using USB communication, via the I^2C protocol, and with an integrated modular software package developed at the Gray Cancer Institute (University of Oxford, United Kingdom) by P. Barber and G. Pierce.

Cells were plated on a SmartSlide-6 Microincubator multiwell plate with heated base and lid (Labtech International, East Sussex, United Kingdom) and temperature and gas were controlled by the SmartSlide 50 system instrument (WaferGen Biosystems, Fremont, CA). Cells were imaged using a 20× Nikon Plan Fluor 0.5 numerical aperture air objective. Images were captured with a Hammatsu Orca charge-coupled device camera every 10 min and analyzed with IrfanView (freeware; www.irfanview.com), ImageJ (National Institutes of Health, Bethesda, MD), and Openlab 5.0.2 software (Improvision, Coventry, United Kingdom).

Western Blot Analysis

Cell extracts, as well as virion lysates, were separated on 10 or 12% polyacrylamide gels and transferred to nitrocellulose membranes. The blots were sequentially probed with monoclonal antibodies α-HIV-1 p24 (183-H12-5C), α-GFP (Roche Diagnostics), or α-TSG101 (4A10; Abcam, Cambridge, United Kingdom), rabbit polyclonal antibodies α-IST1 (ProteinTech Group, Chicago, IL; catalog no. 51002-1-Ap), α-CEP55 (A01; Abnova, Heidelberg, Germany), or α-HSP90 (Santa Cruz Biotechnology) and with a peroxidase-conjugated antibody against mouse (Cell Signaling Technology) or rabbit (Cell Signaling Technology) and developed using chemiluminescent substrate reagents (Pierce Chemical, Rockford, IL).

RESULTS

Identification of hIST1 as a Conserved VPS4-binding Protein

The role of the class E VPS pathway during sorting of ubiquitinated cargo into the nascent vesicles of the MVB is highly conserved in eukaryotic organisms from yeast to mammals. Accordingly, most of the subunits of ESCRT-I, -II, and -III and associated proteins, including VPS4 and ALIX, present a high degree of amino acid sequence similarity, and the comparison of protein–protein interactions within the yeast and human pathways shows that there is also a high degree of conservation at this level (Martin-Serrano *et al*., 2003; Strack *et al*., 2003; von Schwedler *et al*., 2003; Bowers *et al*., 2004). We took advantage of genome-wide screens by yeast two-hybrid and biochemical purification approaches in multiple organisms to identify conserved proteins that interact with VPS4. We first noticed the interaction of *Drosophila melanogaster* VPS4 with CG10103, a protein of unknown function (Giot *et al*., 2003). CG10103 is a homologue of the *Saccharomyces cerevisiae* protein Ist1, a protein that had also been shown to physically interact with Vps4 in yeast by tandem affinity purification (Krogan *et al*., 2006). Sequence analysis showed that Ist1 is well conserved in eukaryotic organisms (Figure 1A), and the human homologue of Ist1 was identified as KIAA0174 (hIST1), with a very conserved N-terminal region and a cluster of conserved amino-acids at the C terminus. Last, a preliminary analysis of expression by expressed sequence tag profile (National Center for Biotechnology Information Unigene) suggested that hIST1 is ubiquitously expressed in human tissues. Sequence analysis indicated that there are four predicted isoforms of KIAA0174: hIST1a (IMAGE Id: 6502833), hIST1b (IMAGE Id: 2819828), hIST1c (IMAGE Id: 6009274), and hIST1d (IMAGE Id: 3350789). When overexpressed in HeLa cells as untagged proteins, hIST1a showed the same molecular weight as the most prominent endogenous protein (data not shown); so, although similar results were obtained with the other isoforms, all the data presented in this study refer to hIST1a.

The interaction of hIST1 with the components of the ESCRT machinery was initially studied by yeast two-hybrid analysis, and binding to VPS4 was observed (Figure 1B). Interestingly, hIST1 also bound to LIP5, a protein involved in VPS4 regulation, and to CHMP1A and CHMP1B, proteins proposed to promote the association of VPS4 with endosomal membranes (Lottridge *et al*., 2006; Nickerson *et al*., 2006). The positive interactions obtained by yeast two-hybrid assays were confirmed using a GST coprecipitation procedure in which a YFP-hIST1 fusion plasmid was cotransfected with plasmids encoding CHMP1A, CHMP1B, VPS4, or LIP5

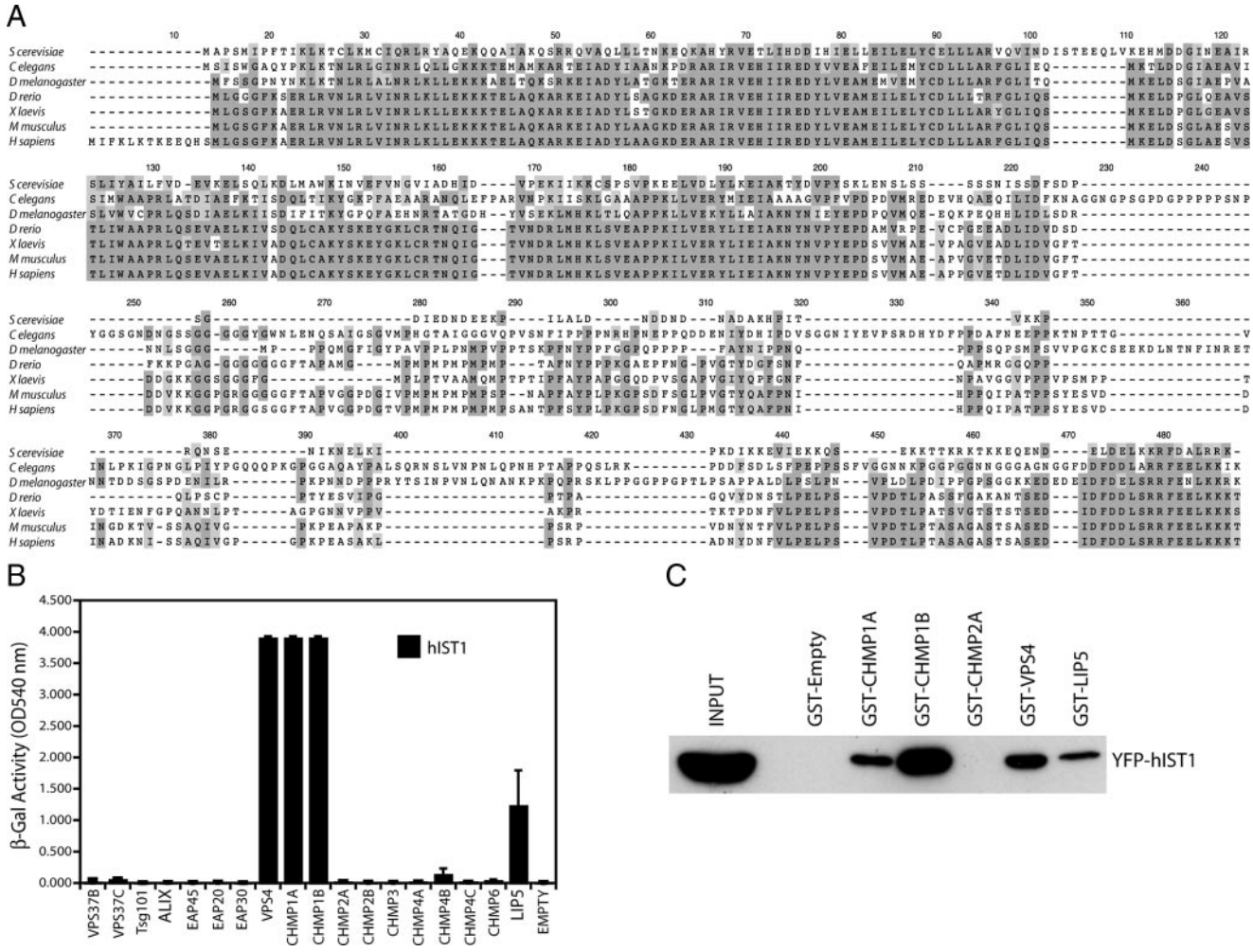

Figure 1. hIST1 binds to CHMP1A, CHMP1B, VPS4, and LIP5. (A) Sequence alignment showing the high degree of similarity between IST1 genes from different organisms. The shading on the alignment indicates conserved amino acids. (B) hIST1 fused to the VP16 activation domain was tested for interactions with the human components of ESCRT-I, -II, -III, and ESCRT-III–associated proteins by yeast two-hybrid assays. Error bars indicate the SD from the mean of triplicate measurements. (C) Coprecipitation assays showing binding of hIST1 to CHMP1A, CHMP1B, CHMP2A, VPS4, and LIP5. One percent of the starting cell lysate (INPUT) and 10% of the volume eluted from the beads were analyzed by Western blot with α-GFP antibody.

fused to GST (Figure 1C). As negative controls, binding of YFP-hIST1 to GST or GST-CHMP2A was undetectable. The interaction was also confirmed in similar coprecipitation assays in which only the GST fusion proteins were transfected, and endogenous hIST1 binding was detected with an α-hIST1 antibody (Supplemental Figure S1).

Mapping the Interactions of hIST1 with the ESCRT Machinery

The structure of CHMP1B has been predicted by analogy with CHMP3 as a core structure formed by a long helical hairpin (formed by helixes α1 and -α2) that together with two short helices forms a four-helical bundle, connected to a fifth helical segment that is positioned perpendicularly to the core (Muziol *et al.*, 2006). At the C terminus, a VPS4-binding region containing the MIM also regulates inhibitory intramolecular interactions (Zamborlini *et al.*, 2006; Obita *et al.*, 2007; Stuchell-Brereton *et al.*, 2007). To characterize the function of hIST1, we first mapped its interaction with CHMP1B by using yeast two-hybrid assays (Figure 2A). Binding to CHMP1A was used as a control for expression and functionality of the different CHMP1B-deleted proteins. This analysis showed that residues 1-61, containing the α1 helix and the N-terminal half of α2 of CHMP1B, are dispensable for binding hIST1. Importantly, the CHMP1B mutant lacking the entire C-terminal regulatory region (CHMP1B 1-156 in Figure 2A) was still able to bind hIST1, showing that hIST1 and VPS4 have distinct binding sites in CHMP1B. A further deletion of CHMP1B containing the amino acids 1-131 failed to bind hIST1, suggesting a requirement of α5 (residues 132-156) for this interaction, although a deleterious effect in the folding of the CHMP1B helical core cannot be excluded from these results.

The structural organization of VPS4 presents an N-terminal MIT domain that mediates recruitment to the ESCRT-III lattice, two AAA ATPase domains and a three-stranded antiparallel β domain that regulates VPS4 activity by binding to LIP5 (or its yeast orthologue Vta1) (Scott *et al.*, 2005; Takasu *et al.*, 2005). Our initial mapping experiments showed that the MIT domain of VPS4 is required for its interaction with hIST1 (Figure 2B, VPS4ΔMIT), suggesting a role for hIST1 in the regulation of VPS4 recruitment by

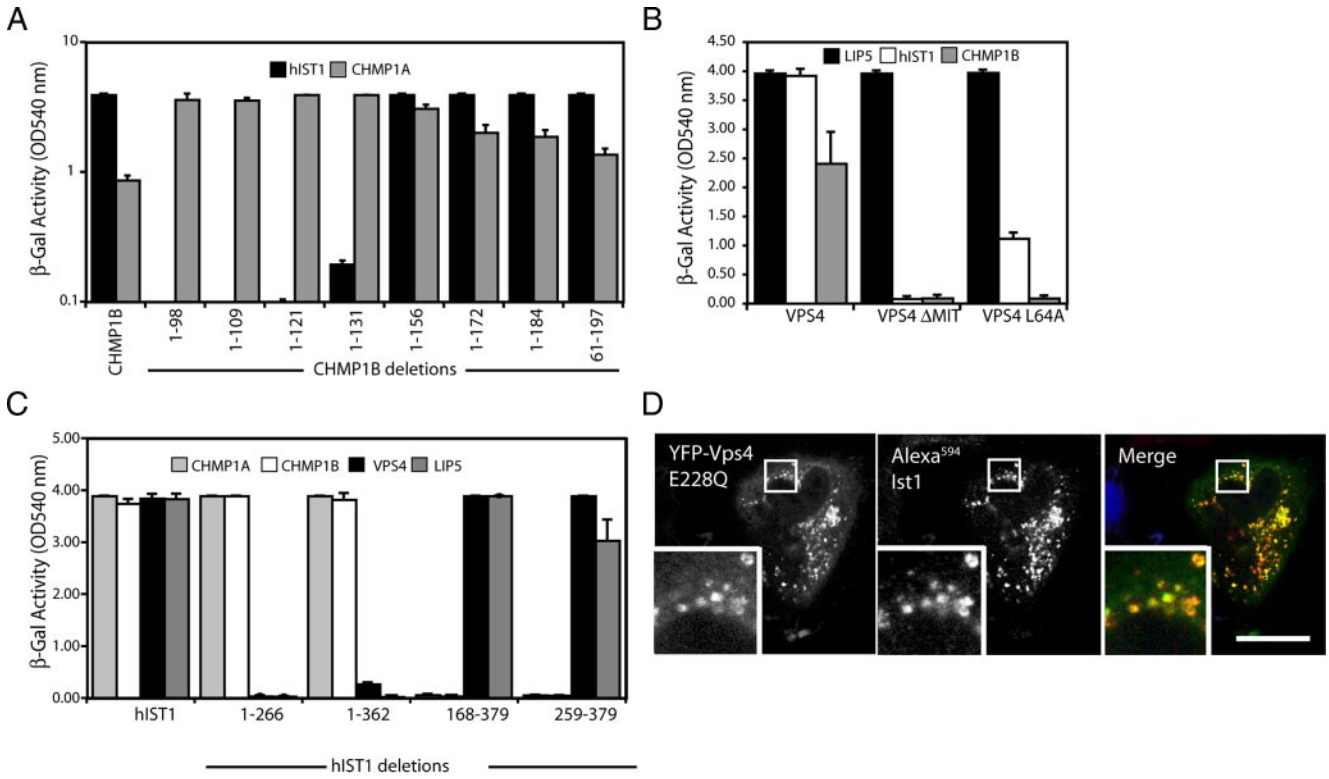

Figure 2. (A) Mapping by yeast two-hybrid analysis of the regions needed in CHMP1B for interaction with IST1. Binding to CHMP1A was used as a positive control; the regions of VPS4 required for interaction with IST1. LIP5 was used as a positive control (B); and the regions of IST1 required for interaction with CHMP1A, CHMP1B, VPS4, or LIP5 (C). Error bars indicate the SD from the mean of triplicate measurements. (D) Micrographs showing that endogenous hIST1 is recruited to aberrant endosomes in the presence of YFP-VPS4 E228Q. Left, images acquired with YFP (pseudocolored in green); middle, images acquired with Alexa594 (pseudocolored in red); and right, overlaid images. A higher magnification of the boxed areas is shown in all panels and DNA is shown in blue. Bar, 10 μm.

ESCRT-III. In agreement with this notion, mutation of a residue in the VPS4 MIT–ESCRT-III interface (VPS4 L64A), resulted in a specific reduction in binding to hIST1 (Figure 2B), although, in contrast to binding to CHMP1B, binding to hIST1 was not abolished, suggesting that hIST1 and CHMP1B bind to VPS4 at overlapping but not identical surfaces of the MIT domain. We then generated hIST1 deletions and tested them for binding to CHMP1A, CHMP1B, VPS4, and LIP5 (Figure 2C). These experiments showed that binding to CHMP1A, -1B clearly segregated from binding to VPS4 and LIP5. Thus, binding to CHMP1A, -1B was mapped to the N-terminal part of hIST1, whereas the region required for binding to VPS4 and LIP5 clustered at the C-terminal 17 amino acids of hIST1. A diagram summarizing hIST1 and CHMP1B mapping studies is shown in Figure 3E.

To complement these interaction studies, the colocalization of hIST1 with the ESCRT machinery was examined by confocal microscopy showing that, at moderate levels of expression, catalytically inactive VPS4 (YFP-VPS4 E228Q) colocalized with endogenous hIST1 in the aberrant endosomal structures induced by YFP-VPS4 E228Q (Figure 2D), indicating that hIST1 is a component of the ESCRT machinery.

hIST1 Encodes a Functional MIM

Results in Figure 2B showed that hIST1 binds to the MIT domain of VPS4 and that mutation of residues in VPS4 involved in the interaction with MIMs also impaired binding to hIST1. The mapping studies in Figure 2C also showed that 17 amino acids at the C terminus of hIST1 are required for binding to VPS4. A closer look at this region showed a predicted helical structure and a significant sequence similarity with a recently described amino-acid motif at the C terminus of several ESCRT-III subunits that binds to the VPS4 MIT domain, namely, MIM (Obita *et al*., 2007; Stuchell-Brereton *et al*., 2007). Importantly, the amino acids in ESCRT-III that contact directly the VPS4 MIT domain are mostly conserved in the putative MIM of both yeast and human IST1 (Figure 3A). To test whether the hIST1 MIM is functional, GST coprecipitation assays were used to test the interaction of hIST1 with several known MIT-containing proteins such as AMSH, UBPY, MITD1, and Spastin. As shown in Figure 3B, full-length hIST1 bound to all the tested proteins containing MIT domains and, as controls, it also bound to VPS4 and the isolated MIT domain of VPS4. Significantly, mutation of amino acids at positions +2 and +3 to alanine in the hIST1 MIM (hIST1 L375A/K376A) abrogated binding to LIP5, MITD1, and UBPY (Figure 3C), whereas binding to CHMP1A and CHMP1B was unaffected. The L375A/K376A mutation also reduced binding to VPS4, although a significant residual binding was still observed, suggesting additional requirements for the hIST1–VPS4 interaction, in agreement with results in Figure 2B and with a recent report suggesting that hIST1 encodes a second, "MIM2," motif that interacts with MIT domains (Kieffer *et al*., 2008). More direct evidence supporting the notion that the C terminus of hIST1 encodes a functional MIM is presented in Figure 3D, showing that amino acids 363-379 of hIST1 are sufficient for binding proteins that contain MIT domains, including LIP5, VPS4, MITD1, and UBPY, whereas

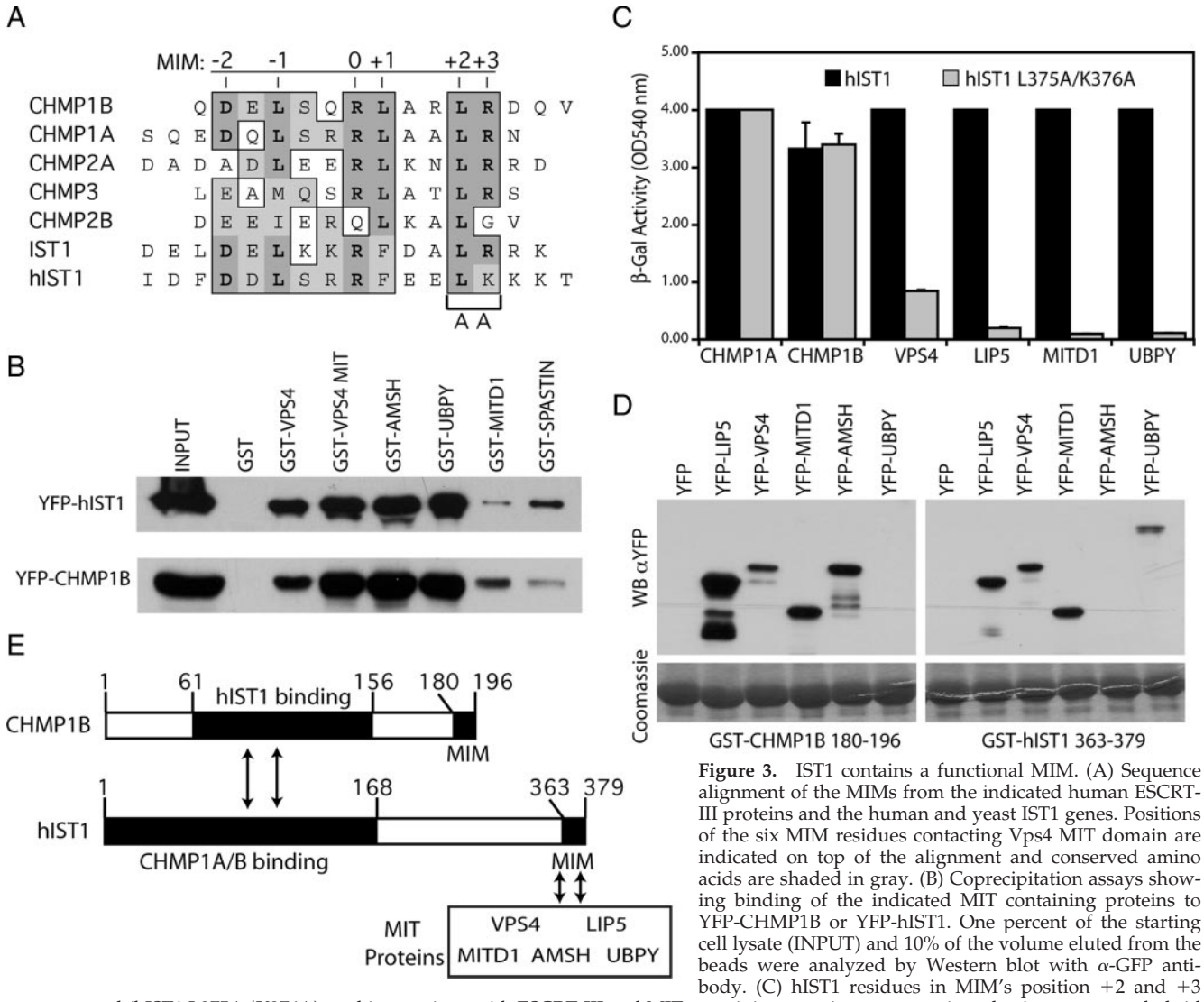

Figure 3. IST1 contains a functional MIM. (A) Sequence alignment of the MIMs from the indicated human ESCRT-III proteins and the human and yeast IST1 genes. Positions of the six MIM residues contacting Vps4 MIT domain are indicated on top of the alignment and conserved amino acids are shaded in gray. (B) Coprecipitation assays showing binding of the indicated MIT containing proteins to YFP-CHMP1B or YFP-hIST1. One percent of the starting cell lysate (INPUT) and 10% of the volume eluted from the beads were analyzed by Western blot with α-GFP antibody. (C) hIST1 residues in MIM's position +2 and +3 were mutated (hIST1 L375A/K376A), and interactions with ESCRT-III and MIT-containing proteins were monitored using yeast two-hybrid assays. Error bars indicate the SD from the mean of triplicate measurements. (D) Cell lysates from bacteria expressing CHMP1B's MIM (GST-CHMP1B 180-196) or hIST1's MIM (GST-hIST1 363-379) were tested by coprecipitation assays for binding to the indicated MIT-containing proteins fused to YFP and binding was monitored with α-GFP mAb (WBαYFP). Bottom, GST fusion protein expression in cell lysates with Coomassie staining. (E) Schematic representation of CHMP1B and hIST1 proteins, showing the regions needed for their interaction (arrows), and the position of their MIMs.

it bound poorly to AMSH. Similar experiments with the CHMP1B MIM (GST-CHMP1B 180-196) showed binding to LIP5, VPS4, MITD1, and AMSH but not to UBPY. Because full-length CHMP1B and hIST1 show no apparent differences in binding to AMSH and UBPY (Figure 3B), it is possible that there are other binding sites outside the MIM needed for the interaction of these proteins. Alternatively, there might be some degree of specificity in the MIT domains that are bound by different MIMs, and this hypothesis will be further investigated.

Characterization of the Function of the IST1 Genes in the MVB Sorting Pathway

In a first step to characterize the function of hIST1, we tested its binding by yeast two-hybrid analysis to the yeast homologues of VPS4 (Vps4), CHMP1A/B (Vps46, also known as Did2 or Fti1), and LIP5 (Vta1). These experiments showed that, like its homologue in *S. cerevisiae*, hIST1 binds to Vps4, Vps46, and Vta1 (Supplemental Figure S3). Moreover, an interaction of yeast Ist1 with human VPS4, CHMP1A, -1B, and LIP5 was also observed (Supplemental Figure S3). Together, these results demonstrate a conserved interaction of IST1 genes with the ESCRT machinery and suggest a conserved function of these genes in eukaryotic organisms.

Two recent studies have investigated the interaction of yeast Ist1 with the ESCRT machinery and its role in Vps4 regulation (Dimaano *et al.*, 2008; Rue *et al.*, 2008). We also tested the effect of *IST1* deletion on the trafficking of a panel of endosomal cargoes and found no obvious trafficking defects in yeast lacking Ist1 (Supplemental Figure S4), confirming that Ist1 is not an essential component of the MVB sorting pathway. Additional characterization of *ist1*Δ revealed that *IST1* is dispensable for cell growth, as shown in a growth curve in Supplemental Figure S3, and deletion of

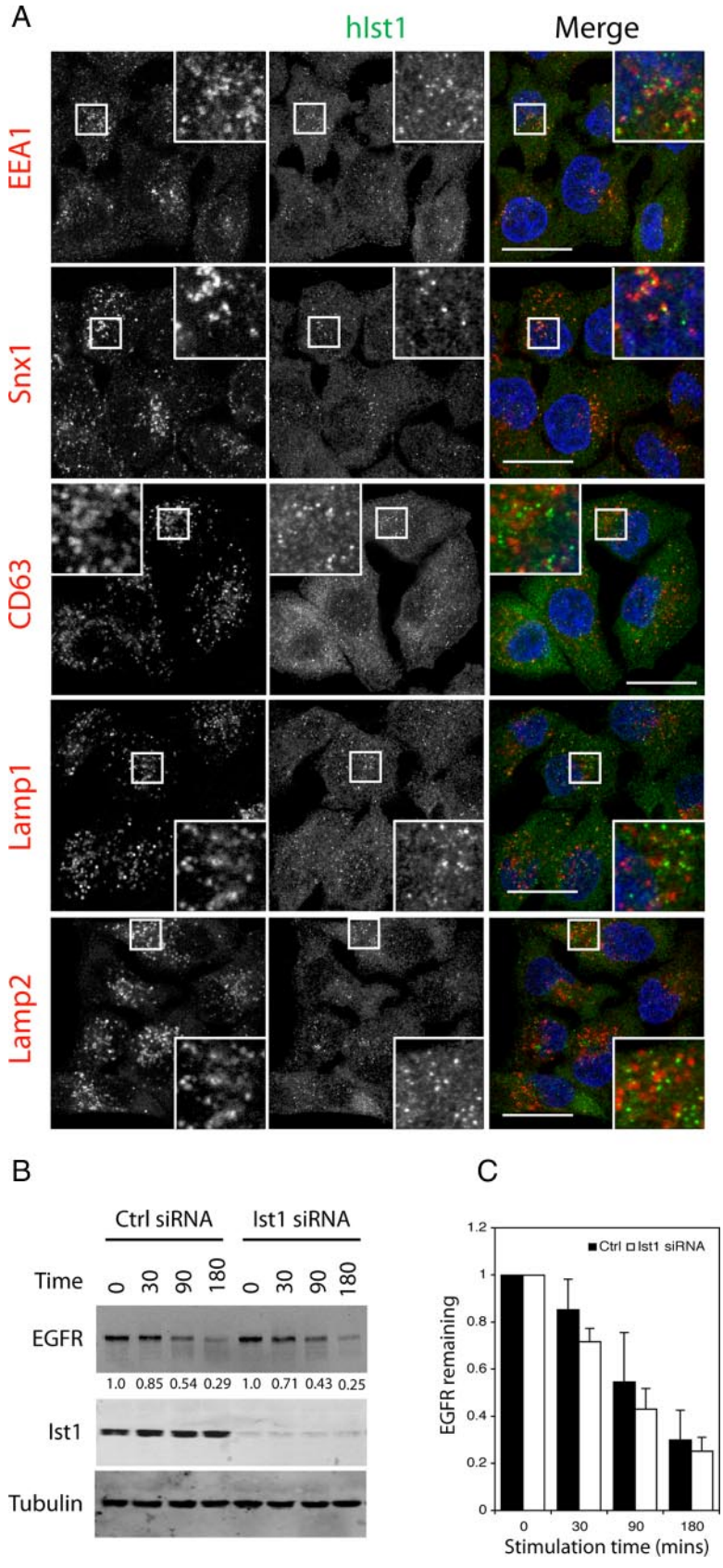

Figure 4. Analysis of hIST1's function in endosomal sorting. (A) Endogenous hIST1 (pseudocolored in green, middle column) and the indicated endosomal markers (pseudocolored in red, left column) were studied by immunofluorescence. A higher magnification of the boxed areas is shown in all panels, and DNA is shown in blue. Bar, 10 μm. (B) HeLa cells treated with either nonspecific control or hIST1-specific siRNA were serum starved and stimulated for the indicated times with EGF. Lysates were analyzed with α-EGFR, α-hIST1, and α-tubulin. (C) Graphic representation of the quantification obtained via infrared imaging after immunoblotting with α-EGFR. Error bars indicate the SD from the mean of triplicate measurements.

IST1 does not result in an increased sodium tolerance in our strains (Supplemental Figure S5). Finally, as shown in Supplemental Figure S3 and in agreement with previous reports (Dimaano *et al*., 2008; Rue *et al*., 2008), *ist1*Δ*vta1*Δ yeast show

enhanced trafficking defects than in either single deletion strain, demonstrating that Ist1 is a positive modulator of the ESCRT machinery.

If hIST1 is involved in cargo sorting at the MVB, we would expect it to associate with late endosomes. We next examined by immunofluorescence the colocalization of endogenous hIST1 with the markers for early endosomes, endogenous early embryonic antigen 1 (EEA1) and Sorting nexin 1 (Snx1) as well as the markers for late endosomes, CD63, and Lamp1 and Lamp2. As shown in Figure 4A, hIST1 accumulates in intracellular punctae that display juxtaposition, but not definitive colocalization, with EEA1 and Snx1. Moreover, no hIST1 was found colocalizing with any of the late endosomal markers that we tested. As shown above (Figure 2D), hIST1 is recruited to endosomal membranes by a dominant-negative mutant of VPS4, suggesting that hIST1 can associate transiently with the endocytic pathway, but the colocalization data with several endosomal markers, suggest that hIST1 does not normally form a sorting complex on the surface of the late endosomes.

Given the role of the ESCRT machinery in receptor downregulation, we tested the function of hIST1 in this process by studying the degradation of the EGF receptor upon activation by EGF in hIST1-depleted cells. As shown in Figure 4B, depletion by siRNA of hIST1 had no effect in EGFR degradation. Importantly, under the same experimental conditions, depletion of hIST1 had a marked effect in cytokinesis (see below; Figure 6) showing that the lack of phenotype in EGFR degradation is not due to a lack of depletion of the endogenous hIST1 protein. Together, these results show that hIST1 is not involved in sorting of ubiquitinated cargo to the MVBs.

hIST1 Is Not Required for HIV-1 Budding

Retroviral budding studies are a good model to investigate the requirement of ESCRT-III and VPS4 in membrane fission because these viruses hijack the cellular components of the MVB protein sorting pathway to facilitate viral release (Morita and Sundquist, 2004). Thus, to determine the possible function of hIST1 in ESCRT-related processes, we followed a dominant-negative approach in which truncations of hIST1 fused to YFP were cotransfected with an HIV-1 provirus in 293T cells, and effects on virus release were measured. As shown in Figure 5A, a C-terminal deletion of hIST1 that does not contain the MIM (YFP-hIST1 1-362), strongly inhibited virus release, indicating that hIST1 overexpression can negatively regulate the pathway's activity and HIV-1 release. Importantly, the effect in virus production is not due to cellular toxicity because overexpression of YFP-hIST1 1-362 did not inhibit Gag expression, but it did induce Gag-processing defects characteristic of L-domain inhibition, as can be seen for the appearance of the cleavage intermediate p25 CA-SP1.

To characterize in more detail the role of hIST1 in HIV-1 budding, a knockdown approach by siRNA was followed. As shown in Figure 5B, specific depletion of endogenous hIST1 did not have an effect in infectious viral release, whereas depletion of TSG101, an ESCRT component essential for viral egress, resulted in a severe reduction of infectious HIV-1 production as reported previously (Garrus *et al.*, 2001). This result was observed for siRNA oligos that knockdown all hIST1 isoforms in the cell (Supplemental Figure S2). Overall, these results show that hIST1 is not essential for viral budding and suggest that the dominant-negative effect exhibited by YFP-hIST1 1-362 might be due to interference with essential components of the ESCRT machinery that are recruited by L-domains.

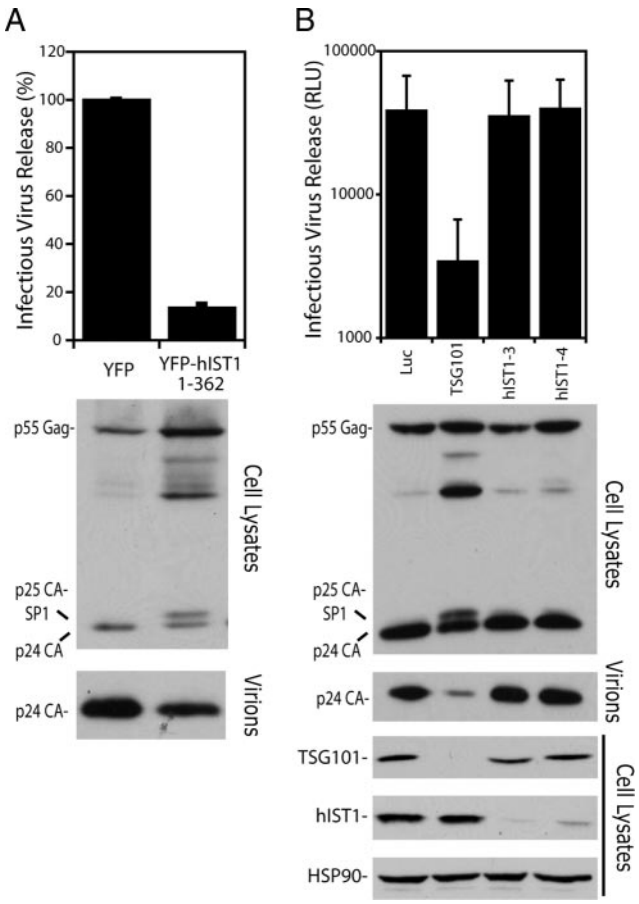

Figure 5. hIST1 effect on HIV budding. (A) Overexpression of a hIST1 fragment lacking the C terminus of the protein fused to YFP inhibits HIV budding. (B) siRNA depletion of endogenous hIST1 has no effect on virus release. TSG101-specific and luciferase control siRNAs were used as positive and negative controls, respectively. Error bars indicate the SD from the mean of three independent experiments. The inhibition of viral particle release was analyzed in cell lysates and extracellular virions by Western blot with α-HIV Gag antibody. The positions on the blot of the precursor Pr55Gag and the mature CA protein are indicated. The bottom images in B show the siRNA-mediated silencing of the endogenous hIST1 and TSG101 and a protein loading control as determined by Western blot analysis with α-TSG101, α-hIST1, and α-HSP90.

hIST1 Is Essential for Cytokinesis in Human Cells

Cytokinesis is an analogous membrane fission event to MVB vesicle formation and virus budding that requires components of the ESCRT machinery. During the last step of cell division, CEP55 acts as an adaptor protein that recruits TSG101 and ALIX to the midbody and depletion of any of these proteins from the cell results in a failure of cytokinesis and, consequently, in an accumulation of multinucleated cells (Carlton and Martin-Serrano, 2007; Morita *et al.*, 2007; Carlton *et al.*, 2008). We decided to investigate the role of hIST1 in this process by siRNA, observing that depletion of hIST1 resulted in an accumulation of multinucleated cells (Figure 6A) as severe as the phenotype observed in CEP55- and ALIX-depleted cells. hIST knockdown also induced an increase of dividing cells with intercellular bridges similar to the increase induced by CEP55 and ALIX depletion, indicating a specific requirement of hIST1 in late events of cytokinesis. Importantly, the percentage of multinucleated cells was significantly restored when siRNA-resistant hIST1 was

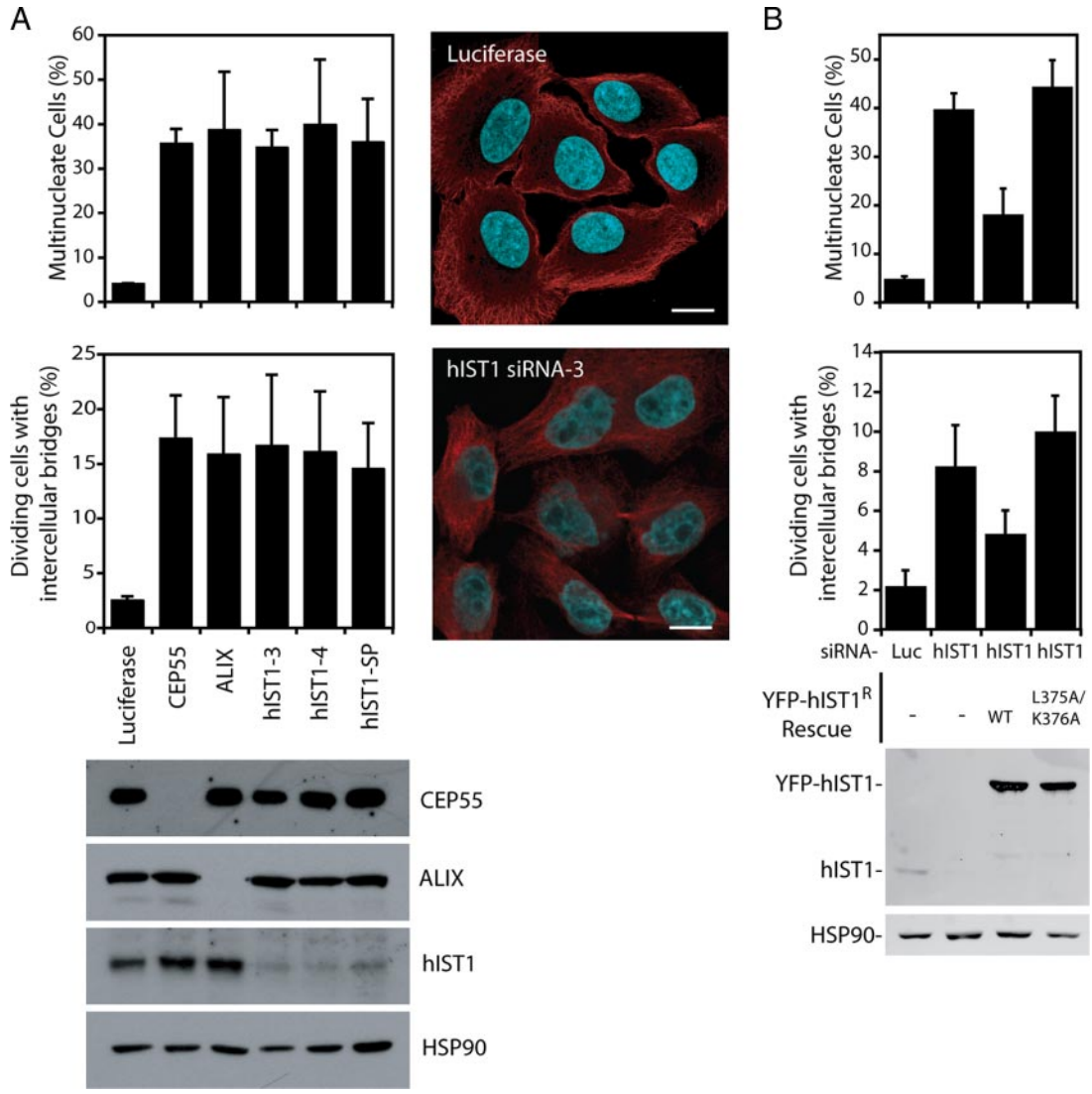

Figure 6. hIST1 is required for cytokinesis. (A) HeLa cells were transfected with siRNA targeting CEP55, ALIX, hIST1 (hIST1-3, hIST1-4, and Dharmacon's siGENOME SMARTpool (hIST1-SP), or a luciferase control and scored for multinucleation. Representative micrographs are shown (B) in which tubulin is labeled in red. HeLa cells stably expressing YFP (−), siRNA-resistant YFP-hIST1 (WT), or siRNA-resistant YFP-hIST1 L375A/K376A were treated with the indicated siRNA and scored for multinucleation or dividing cells with intercellular bridges. Error bars indicate the SD from the mean of triplicate measurements. siRNA-mediated depletion of the indicated endogenous protein was examined by immunoblotting with α-CEP55, α-ALIX, or α-hIST1. Protein loading control was determined with α-HSP90.

reintroduced in the cells (Figure 6B), showing that the cytokinesis defect observed with the siRNA against hIST1 is specific. The slightly higher number of multinucleated cells observed in siRNA-resistant hIST1 expressing cells compared with the control cells might be due to the considerably higher expression levels observed for the RNAi-resistant constructs compared with the endogenous hIST1 levels.

As shown above, hIST1 contains a C-terminal MIM that binds to VPS4, LIP5, and other MIT-containing proteins. To test whether this motif is important for hIST1's function in cytokinesis, we depleted and replaced the endogenous hIST1 with siRNA-resistant hIST1 L375A/K376A, which is unable to bind MIT-containing proteins. As shown in Figure 6B, the cells that rely solely on hIST1 L375A/K376A showed a strong defect in cytokinesis and an increase of dividing cells with intercellular bridges that recapitulates the phenotype observed in cells depleted of the endogenous hIST1. Together, these results show that hIST1 is required for cytokinesis and that its ability to bind and possibly recruit MIT-containing proteins is essential for its function in the last step of cell division. Additional functions at the N terminus of hIST1 are also required for late stages of cell division as suggested by defects in cytokinesis observed in cells expressing hIST1 259-379 (data not shown).

To further characterize the cytokinesis phenotype caused by hIST1 depletion, time-lapse imaging of cell division after siRNA treatment was carried out. We used HeLa cells stably expressing mCherry-Tubulin to identify cells in mitosis and follow the bridge dynamics throughout cytokinesis. Among the cells studied, 90% of the control-treated cells (n = 10), but only 9% of hIST1-knockdown cells (n = 22), underwent successful cytokinesis and completed cell abscission, with an average duration time of 96 min after telophase (Figure 7C). Cleavage furrow ingression was observed in all the hIST1-depleted cells examined. However, in 77.3% of the hIST1-treated cells, the two newly formed daughter cells remained

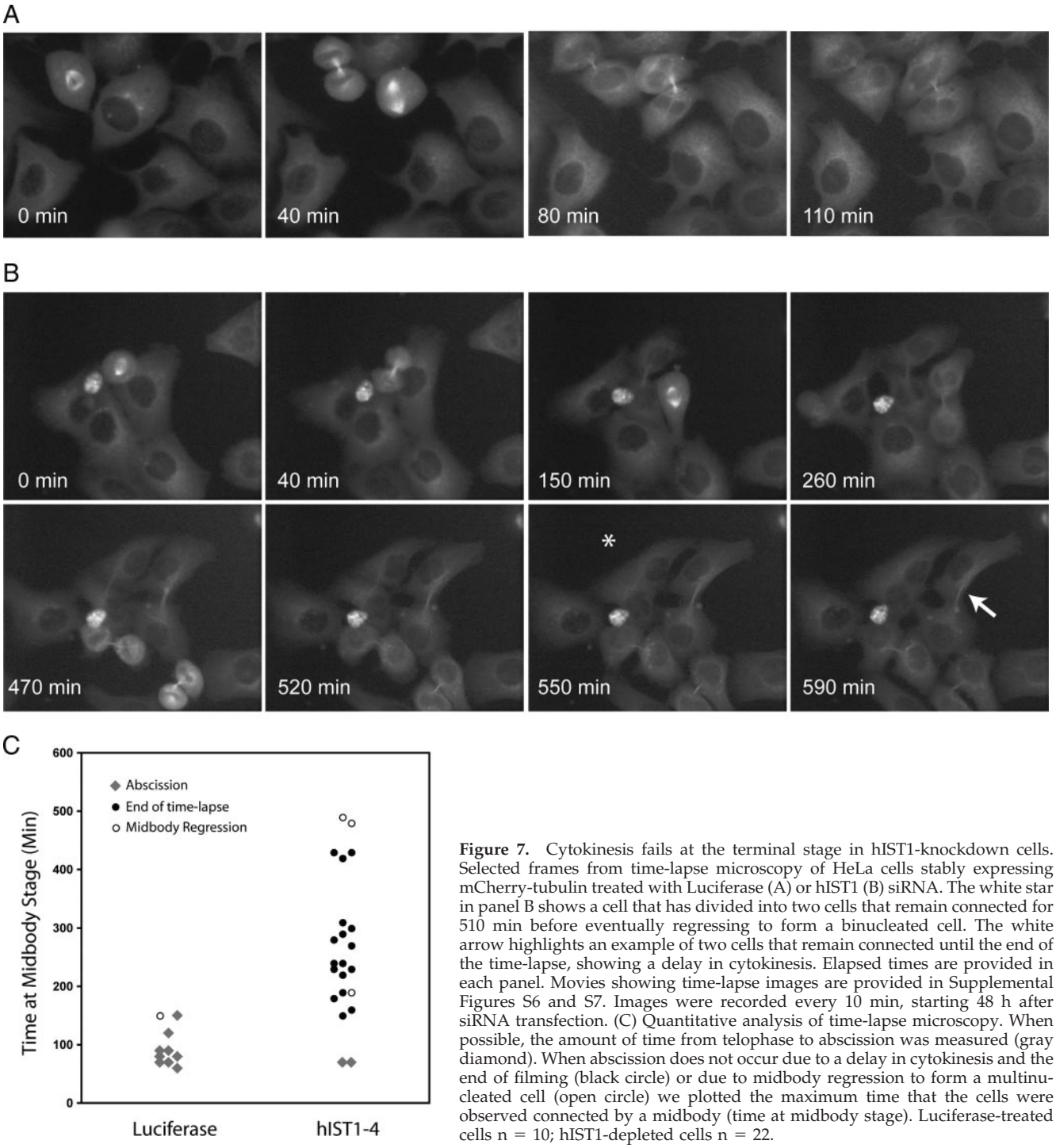

Figure 7. Cytokinesis fails at the terminal stage in hIST1-knockdown cells. Selected frames from time-lapse microscopy of HeLa cells stably expressing mCherry-tubulin treated with Luciferase (A) or hIST1 (B) siRNA. The white star in panel B shows a cell that has divided into two cells that remain connected for 510 min before eventually regressing to form a binucleated cell. The white arrow highlights an example of two cells that remain connected until the end of the time-lapse, showing a delay in cytokinesis. Elapsed times are provided in each panel. Movies showing time-lapse images are provided in Supplemental Figures S6 and S7. Images were recorded every 10 min, starting 48 h after siRNA transfection. (C) Quantitative analysis of time-lapse microscopy. When possible, the amount of time from telophase to abscission was measured (gray diamond). When abscission does not occur due to a delay in cytokinesis and the end of filming (black circle) or due to midbody regression to form a multinucleated cell (open circle) we plotted the maximum time that the cells were observed connected by a midbody (time at midbody stage). Luciferase-treated cells n = 10; hIST1-depleted cells n = 22.

connected by an intercellular bridge for >150 min and did not complete cell abscission during the duration of the time-lapse imaging (Figure 7C). These data suggest that hIST1-knockdown cells fail at late stages of cytokinesis and that the intercellular bridge is very stable. Additionally, in 13.7% of the hIST1 siRNA-treated cells, midbodies regressed after remaining interconnected for extended time (an average of 396 min) to become a binucleated cell (Figure 7C). A representative example of bridge regression occurring 510 min after telophase is shown in Figure 7B (movie in Supplemental Figure S7), and an example of a control cell is shown in Figure 7A (movie in Supplemental Figure S6). These results and the accumulation of cells connected by the intercellular bridge in cells depleted of hIST1 (Figure 6A) support a defect in abscission and argue against defects in furrow ingression or midbody stability defects.

hIST1 Localizes to the Midbody in Cytokinesis

The role of hIST1 in cytokinesis prompted us to examine by immunofluorescence staining the subcellular distribution of endogenous hIST1 in HeLa cells during the different phases of mitosis. As shown in Figure 8, hIST1 exhibits a localiza-

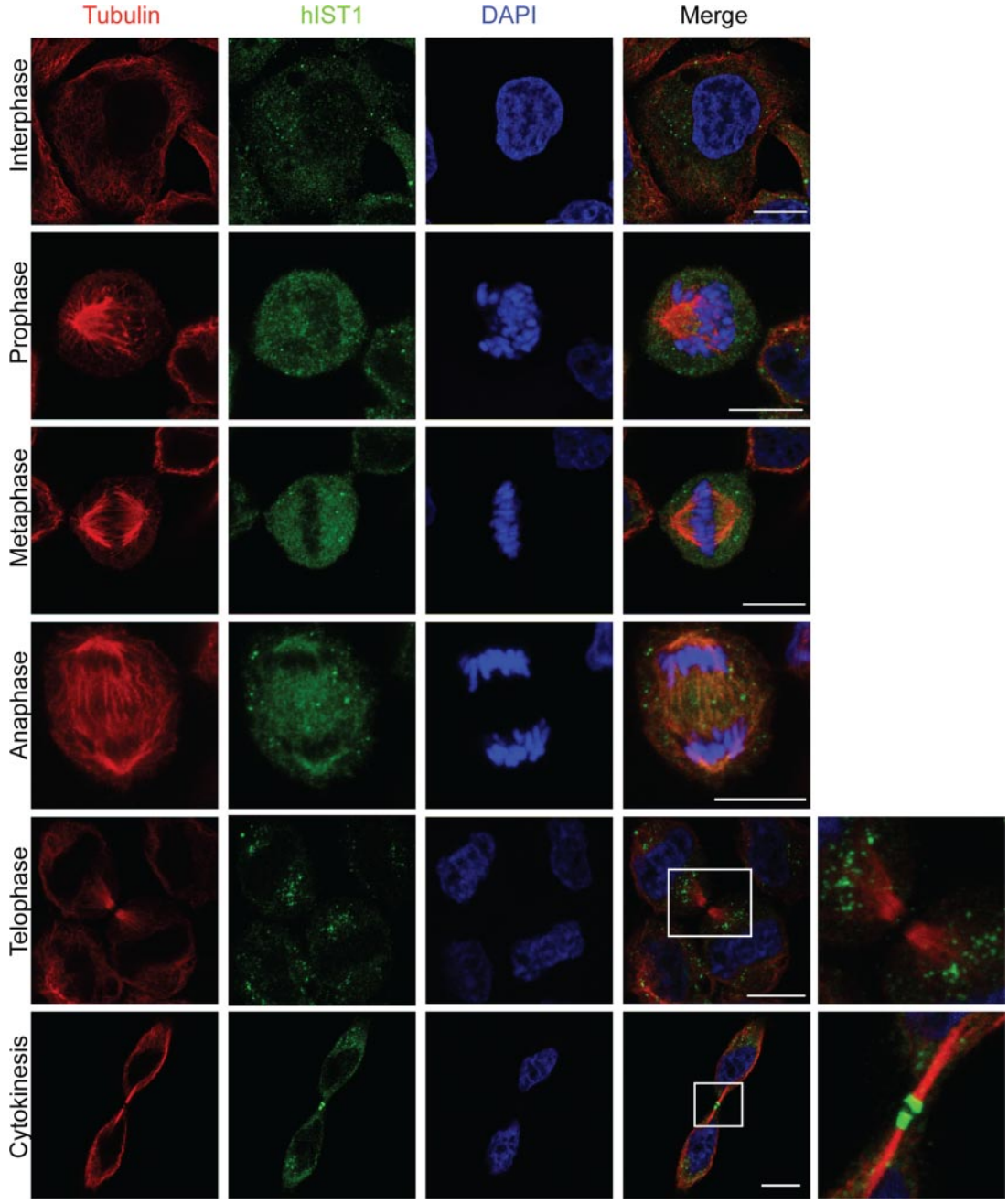

Figure 8. Cellular localization of endogenous hIST1 during mitosis in human HeLa cells. hIST1 accumulates near the spindle during telophase and is detected at the midbody during cytokinesis. HeLa cells were immunostained for hIST1 (green), α-tubulin (red) and DNA (blue). The far right column shows a higher magnification of the boxed areas in the merged column of cells in telophase and cytokinesis. Bar, 10 μm.

tion that is mainly cytosolic with some accumulation in punctate structures. Interestingly, no obvious accumulation of the protein during mitosis was seen until telophase, in which hIST1 relocalizes considerably and accumulates near the microtubules that form the spindle. Importantly, a clear localization of hIST1 at the midbody was mostly observed in later stages of cytokinesis, which is consistent with a role of hIST1 in abscission (Figure 8). Interestingly, hIST1's relocalization to the midbody during cytokinesis is similar to that observed previously for VPS4A (Morita *et al*., 2007), a binding partner of hIST1.

Characterization of the Intercellular Bridge in Cells Depleted of hIST1

Because hIST1 localizes to the midbody and is needed for cytokinesis, we examined whether hIST1 is required for the recruitment of several components of the midbody structure. As shown in Figure 9, A and B, immunofluorescence studies determined that components of the Flemming body and the midbody ring, such as CEP55, AuroraB, and MKLP1 (Guse *et al*., 2005; Zhao *et al*., 2006), are present at the midbody after hIST1 depletion. Importantly, Tsg101 and Alix, two components of the ESCRT machinery that are

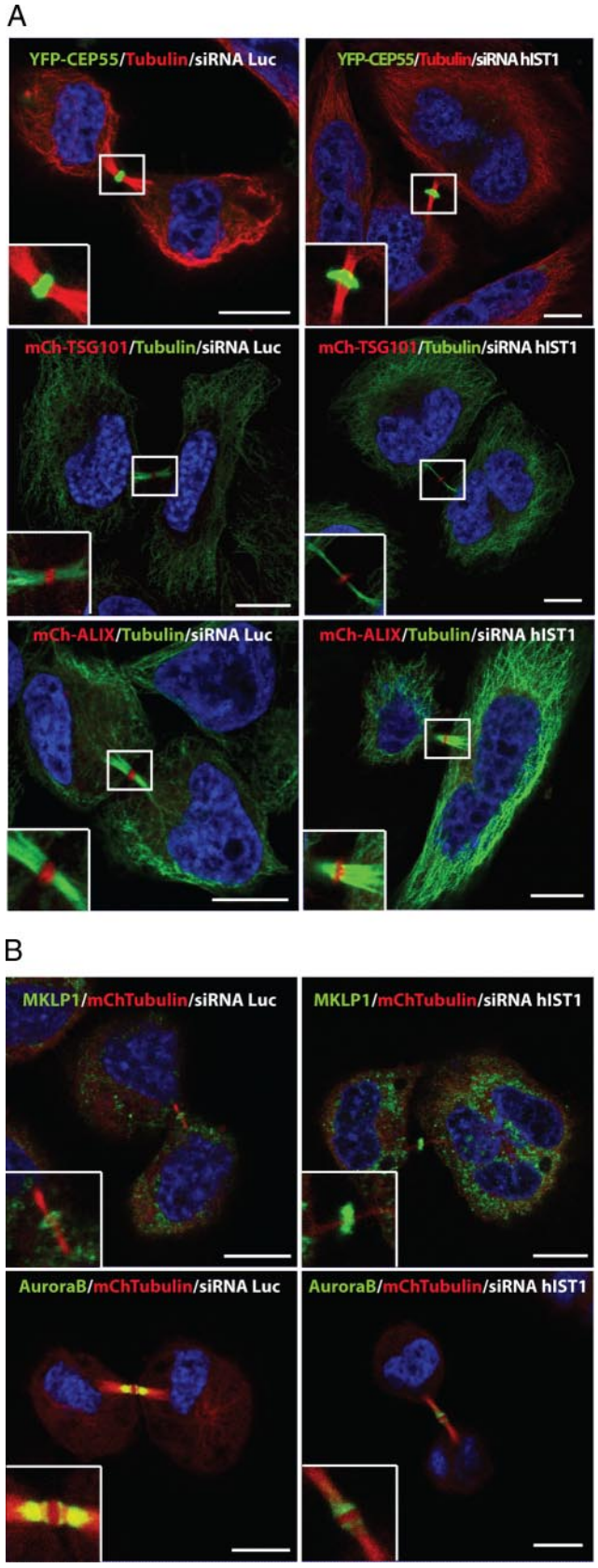

Figure 9. Characterization of the midbody composition in cells that lack hIST1. (A) Representative micrographs describing midbody localization of YFP-CEP55 (green), mCh-TSG101 (red), or mCh-ALIX (red) in cells stably expressing these fusion proteins and treated with siRNA targeting luciferase or hIST1. After siRNA treatment, cells were fixed and stained with α-tubulin and Alexa594 (red) or Alexa488 (green) conjugated secondary antibodies. (B) Similarly, HeLa cells stably expressing mCh-Tubulin (red) treated with siRNA targeting luciferase or hIST1 were immunostained for MKLP1 or AuroraB (green). In all cases, enlargements depict the midbody localization of the studied proteins. DNA is shown in blue. Bar, 10 μm.

required during late stages of cytokinesis, are also recruited to the Flemming body after hIST1 depletion (Figure 9B).

DISCUSSION

In the present study, we characterize KIAA0174, a human protein of previously unknown function, as the homologue of *S. cerevisiae* Ist1; thus, we have named it hIST1. We also describe the conserved interaction of hIST1 with several components of the ESCRT machinery, namely, CHMP1A, -1B, VPS4, and LIP5. Remarkably, hIST1 binds the yeast homologues of CHMP1A/B, VPS4 and LIP5, and the converse interactions were also observed with yeast Ist1, suggesting a highly conserved function of IST1 in the ESCRT pathway. In despite of this functional conservation, the data presented in this and other studies (Dimaano *et al*., 2008; Rue *et al*., 2008) show that *ist1*Δ yeasts present no obvious phenotype in endosomal cargo sorting, perhaps explaining why IST1 was not identified in previous genetic screens. The functional studies in human cells also show a nonessential role of hIST1 in endosomal sorting and HIV-1 budding. Interestingly, hIST knockdown by RNAi in mammalian cells has revealed an essential role of hIST1 in late events of cytokinesis, but yeast strains lacking *IST1* or essential components of the ESCRT machinery do not exhibit apparent defects in cell growth, suggesting that the role of *IST1* and the ESCRT complexes may not be conserved in yeast cell division. The high degree of sequence and functional conservation, together with the lack of a phenotype in *ist1*Δ yeasts, raises the possibility that *IST1* might also play an essential role in currently unidentified biological processes other than MVB formation in eukaryotic cells.

The genetic interaction of *IST1* with *VTA1* has been observed in this and recent studies (Dimaano *et al*., 2008; Rue *et al*., 2008), suggesting a role of *IST1* as a positive regulator of the MVB protein sorting pathway. Indeed, extensive genetic analyses suggest that Ist1-Vps46 and Vta1-Vps60 form two separate functional complexes that provide alternative ways to modulate late events during MVB sorting (Rue *et al*., 2008). An additional negative regulation of the cytoplasmic pool of Vps4 by Ist1 has also been reported and a competition of Ist1 with Vta1 for binding Vps4 has been proposed to explain the negative regulation of Vps4 by Ist1 (Dimaano *et al*., 2008). However, the Vta1 structure shows a C-terminal Vps4 binding domain and two N-terminal MIT domains that might be located at the periphery of the Vps4 double ring structure (Xiao *et al*., 2008). We describe here the requirement of the hIST1 MIM in the conserved interaction of hIST1 (Ist1) with LIP5 (Vta1), suggesting a requirement of the Vta1/LIP5 MIT domain in this interaction, thus arguing against a competition of hIST1 and LIP5 for binding VPS4.

The ESCRT-III subunits and ESCRT-III-associated proteins Vps2 and Vps46 in yeast and CHMP1A/B, CHMP2A/B, and CHMP3 in humans have recently been described to contain MIMs (Obita *et al*., 2007; Stuchell-Brereton *et al*., 2007). Interestingly, IST1 is the first non-ESCRT-III protein that contains an MIM, raising the possibility that

additional proteins unrelated to ESCRTs might also encode functional MIMs. Our results show that the hIST1 MIM is essential in cytokinesis, as demonstrated by the finding that a hIST1 MIM mutant (hIST1 L375A/K376A) is not able to rescue the cytokinesis defects induced by siRNA depletion of the endogenous hIST1 (Figure 6). Vps4 activation can occur either through the interaction of its MIT domain with the MIMs found in the ESCRT-III subunits or via the binding of its β-domain to Vta1, providing several modes for ESCRT disassembly (Scott *et al*., 2005; Azmi *et al*., 2006, 2008). In this context, the specific role of hIST1 in cytokinesis might be explained by a direct activation of VPS4 by the hIST1 MIM during late stages of cell division. The mapping studies and the colocalization results shown in Figure 2 suggest that hIST1 can bind simultaneously to CHMP1A/B- and MIT-containing proteins, perhaps providing another mechanism to regulate ESCRT-III disassembly whereby hIST1 might stabilize LIP5-VPS4-ESCRT-III complexes by creating a network of MIMs. Accordingly, MIMs bind MIT domains with a modest affinity ($\sim$30 μM) (Obita *et al*., 2007; Stuchell-Brereton *et al*., 2007) and a network of MIMs, provided both by ESCRT-III and hIST1, might increase the avidity for MIT-containing proteins, such as VPS4 and LIP5, thus increasing the local stability of active VPS4 in the midbody. In agreement with this hypothesis, Ist1 displays synthetic genetic interactions with a Vps2 point mutant in its MIM that renders it unable to bind Vps4 (Rue *et al*., 2008).

In addition to stabilizing the ESCRT–III/VPS4 complex, hIST1 might provide a platform at the midbody to recruit a different array of MIT-containing proteins required for cytokinesis. Interestingly, a recent report shows that overexpression of a catalytically inactive form of one of the MIT-containing proteins that binds to hIST1, namely, UBPY, leads to the appearance of multinucleated cells (Pohl and Jentsch, 2008), perhaps suggesting that ubiquitin modification at the midbody is needed for efficient cytokinesis. We show in this study that deletion of Ist1, Vps4, or other ESCRT components does not result in apparent defects in cell growth in yeast, suggesting that the role of the ESCRT machinery in cytokinesis has been acquired later in evolution. Hence, it will be of great interest to characterize further whether the MIT-containing proteins that bind to hIST1 and do not have a yeast homologue, such as MITD1 or Spastin, provide nonconserved functions needed for late steps in mammalian cell division.

Last, the role of the ESCRT pathway in sorting of ubiquitinated cargo rises the possibility that this machinery might be involved in trafficking events during cytokinesis (Prekeris and Gould, 2008) or, alternatively, it might also be required for selective retrieval of ubiquitinated cargo from the midbody (Van Damme *et al*., 2008). However, based on the evidence presented in this and other reports (Carlton and Martin-Serrano, 2007; Morita *et al*., 2007; Carlton *et al*., 2008), we favor a model whereby the mammalian ESCRT machinery is recruited by different adaptor proteins to facilitate several topologically similar membrane scission events that include abscission. The first level of specificity for the different processes seems to be mediated by the nature of the different adaptor proteins, namely, HRS in endosomal sorting, Gag proteins in viral budding and CEP55 in cytokinesis. A second level of specificity in this pathway would be mediated by the multiple isoforms of some ESCRT components that are present in the human pathway (Carlton *et al*., 2008) and the differential requirement for hIST1 in MVB sorting, HIV-1 budding and mammalian cell division indicates another way of acquiring functional diversification, suggesting that different components of the ESCRT machinery might modulate VPS4 activity and/or other activities of the pathway at specific cellular compartments.

ACKNOWLEDGMENTS

We thank Nathan Sherer for help with the time-lapse microscopy and helpful discussion and Wes Sundquist for generous gift of hIST1 antibody. This work was supported by Career Establishment grant G0400207 from the Medical Research Council UK. J.G.C. is a Beit Memorial Research Fellow.

REFERENCES

Agromayor, M., and Martin-Serrano, J. (2006). Interaction of AMSH with ESCRT-III and deubiquitination of endosomal cargo. J. Biol. Chem. *281*, 23083–23091.

Azmi, I., Davies, B., Dimaano, C., Payne, J., Eckert, D., Babst, M., and Katzmann, D. J. (2006). Recycling of ESCRTs by the AAA-ATPase Vps4 is regulated by a conserved VSL region in Vta1. J. Cell Biol. *172*, 705–717.

Azmi, I. F., Davies, B. A., Xiao, J., Babst, M., Xu, Z., and Katzmann, D. J. (2008). ESCRT-III family members stimulate Vps4 ATPase activity directly or via Vta1. Dev. Cell *14*, 50–61.

Babst, M., Katzmann, D. J., Estepa-Sabal, E. J., Meerloo, T., and Emr, S. D. (2002a). Escrt-III: an endosome-associated heterooligomeric protein complex required for mvb sorting. Dev. Cell *3*, 271–282.

Babst, M., Katzmann, D. J., Snyder, W. B., Wendland, B., and Emr, S. D. (2002b). Endosome-associated complex, ESCRT-II, recruits transport machinery for protein sorting at the multivesicular body. Dev. Cell *3*, 283–289.

Babst, M., Wendland, B., Estepa, E. J., and Emr, S. D. (1998). The Vps4p AAA ATPase regulates membrane association of a Vps protein complex required for normal endosome function. EMBO J. *17*, 2982–2993.

Barr, F. A., and Gruneberg, U. (2007). Cytokinesis: placing and making the final cut. Cell *131*, 847–860.

Bieniasz, P. D. (2006). Late budding domains and host proteins in enveloped virus release. Virology *344*, 55–63.

Bogerd, H. P., Fridell, R. A., Blair, W. S., and Cullen, B. R. (1993). Genetic evidence that the Tat proteins of human immunodeficiency virus types 1 and 2 can multimerize in the eukaryotic cell nucleus. J. Virol. *67*, 5030–5034.

Bowers, K., Lottridge, J., Helliwell, S. B., Goldthwaite, L. M., Luzio, J. P., and Stevens, T. H. (2004). Protein-protein interactions of ESCRT complexes in the yeast *Saccharomyces cerevisiae*. Traffic *5*, 194–210.

Burke, D., Dawson, D., and Stearns, T. (2000). Methods in Yeast Genetics: A Cold Spring Harbor Laboratory Course Manual, New York: Cold Spring Harbor Laboratory Press.

Carlton, J. G., Agromayor, M., and Martin-Serrano, J. (2008). Differential requirements for Alix and ESCRT-III in cytokinesis and HIV-1 release. Proc. Natl. Acad. Sci. USA *105*, 10541–10546.

Carlton, J. G., and Martin-Serrano, J. (2007). Parallels between cytokinesis and retroviral budding: a role for the ESCRT machinery. Science *316*, 1908–1912.

Demirov, D. G., and Freed, E. O. (2004). Retrovirus budding. Virus Res. *106*, 87–102.

Demirov, D. G., Ono, A., Orenstein, J. M., and Freed, E. O. (2002). Overexpression of the N-terminal domain of TSG101 inhibits HIV-1 budding by blocking late domain function. Proc. Natl. Acad. Sci. USA *99*, 955–960.

Derdeyn, C. A., Decker, J. M., Sfakianos, J. N., Wu, X., O'Brien, W. A., Ratner, L., Kappes, J. C., Shaw, G. M., and Hunter, E. (2000). Sensitivity of human immunodeficiency virus type 1 to the fusion inhibitor T-20 is modulated by coreceptor specificity defined by the V3 loop of gp120. J. Virol. *74*, 8358–8367.

Dimaano, C., Jones, C. B., Hanono, A., Curtiss, M., and Babst, M. (2008). Ist1 regulates vps4 localization and assembly. Mol. Biol. Cell *19*, 465–474.

Durocher, Y., Perret, S., and Kamen, A. (2002). High-level and high-throughput recombinant protein production by transient transfection of suspension-growing human 293-EBNA1 cells. Nucleic Acids Res. *30*, E9.

Eggert, U. S., Mitchison, T. J., and Field, C. M. (2006). Animal cytokinesis: from parts list to mechanisms. Annu. Rev. Biochem. *75*, 543–566.

Freed, E. O. (2002). Viral late domains. J. Virol. *76*, 4679–4687.

Garrus, J. E., *et al*. (2001). Tsg101 and the vacuolar protein sorting pathway are essential for HIV-1 budding. Cell *107*, 55–65.

Giot, L., *et al*. (2003). A protein interaction map of *Drosophila melanogaster*. Science *302*, 1727–1736.

Glotzer, M. (2001). Animal cell cytokinesis. Annu. Rev. Cell Dev. Biol. *17*, 351–386.

Gruenberg, J., and Stenmark, H. (2004). The biogenesis of multivesicular endosomes. Nat. Rev. Mol. Cell Biol. *5*, 317–323.

Guse, A., Mishima, M., and Glotzer, M. (2005). Phosphorylation of ZEN-4/MKLP1 by aurora B regulates completion of cytokinesis. Curr. Biol. *15*, 778–786.

Hanson, P. I., Roth, R., Lin, Y., and Heuser, J. E. (2008). Plasma membrane deformation by circular arrays of ESCRT-III protein filaments. J. Cell Biol. *180*, 389–402.

Hurley, J. H., and Emr, S. D. (2006). The ESCRT complexes: structure and mechanism of a membrane-trafficking network. Annu. Rev. Biophys. Biomol. Struct. *35*, 277–298.

Katzmann, D. J., Babst, M., and Emr, S. D. (2001). Ubiquitin-dependent sorting into the multivesicular body pathway requires the function of a conserved endosomal protein sorting complex, ESCRT-I. Cell *106*, 145–155.

Kieffer, C., Skalicky, J. J., Morita, E., De Domenico, I., Ward, D. M., Kaplan, J., and Sundquist, W. I. (2008). Two distinct modes of ESCRT-III recognition are required for VPS4 functions in lysosomal protein targeting and HIV-1 budding. Dev. Cell *15*, 62–73.

Krogan, N. J., *et al*. (2006). Global landscape of protein complexes in the yeast *Saccharomyces cerevisiae*. Nature *440*, 637–643.

Langelier, C., von Schwedler, U. K., Fisher, R. D., De Domenico, I., White, P. L., Hill, C. P., Kaplan, J., Ward, D., and Sundquist, W. I. (2006). Human ESCRT-II complex and its role in human immunodeficiency virus type 1 release. J. Virol. *80*, 9465–9480.

Lottridge, J. M., Flannery, A. R., Vincelli, J. L., and Stevens, T. H. (2006). Vta1p and Vps46p regulate the membrane association and ATPase activity of Vps4p at the yeast multivesicular body. Proc. Natl. Acad. Sci. USA *103*, 6202–6207.

Martin-Serrano, J. (2007). The role of ubiquitin in retroviral egress. Traffic *8*, 1297–1303.

Martin-Serrano, J., Yarovoy, A., Perez-Caballero, D., and Bieniasz, P. D. (2003). Divergent retroviral late-budding domains recruit vacuolar protein sorting factors by using alternative adaptor proteins. Proc. Natl. Acad. Sci. USA *100*, 12414–12419.

Martin-Serrano, J., Zang, T., and Bieniasz, P. D. (2001). HIV-1 and Ebola virus encode small peptide motifs that recruit Tsg101 to sites of particle assembly to facilitate egress. Nat. Med. *7*, 1313–1319.

McCullough, J., Row, P. E., Lorenzo, O., Doherty, M., Beynon, R., Clague, M. J., and Urbe, S. (2006). Activation of the endosome-associated ubiquitin isopeptidase AMSH by STAM, a component of the multivesicular body-sorting machinery. Curr. Biol. *16*, 160–165.

Morita, E., Sandrin, V., Chung, H. Y., Morham, S. G., Gygi, S. P., Rodesch, C. K., and Sundquist, W. I. (2007). Human ESCRT and ALIX proteins interact with proteins of the midbody and function in cytokinesis. EMBO J. *26*, 4215–4227.

Morita, E., and Sundquist, W. I. (2004). Retrovirus budding. Annu. Rev. Cell Dev. Biol. *20*, 395–425.

Muziol, T., Pineda-Molina, E., Ravelli, R. B., Zamborlini, A., Usami, Y., Gottlinger, H., and Weissenhorn, W. (2006). Structural basis for budding by the ESCRT-III factor CHMP3. Dev. Cell *10*, 821–830.

Nickerson, D. P., West, M., and Odorizzi, G. (2006). Did2 coordinates Vps4-mediated dissociation of ESCRT-III from endosomes. J. Cell Biol. *175*, 715–720.

Obita, T., Saksena, S., Ghazi-Tabatabai, S., Gill, D. J., Perisic, O., Emr, S. D., and Williams, R. L. (2007). Structural basis for selective recognition of ESCRT-III by the AAA ATPase Vps4. Nature *449*, 735–739.

Pohl, C., and Jentsch, S. (2008). Final stages of cytokinesis and midbody ring formation are controlled by BRUCE. Cell *132*, 832–845.

Prekeris, R., and Gould, G. W. (2008). Breaking up is hard to do—membrane traffic in cytokinesis. J. Cell Sci. *121*, 1569–1576.

Roberts, C. J., Raymond, C. K., Yamashiro, C. T., and Stevens, T. H. (1991). Methods for studying the yeast vacuole. Methods Enzymol. *194*, 644–661.

Row, P. E., Liu, H., Hayes, S., Welchman, R., Charalabous, P., Hofmann, K., Clague, M. J., Sanderson, C. M., and Urbe, S. (2007). The MIT domain of UBPY constitutes a CHMP binding and endosomal localization signal required for efficient epidermal growth factor receptor degradation. J. Biol. Chem. *282*, 30929–30937.

Rue, S. M., Mattei, S., Saksena, S., and Emr, S. D. (2008). Novel ist1-did2 complex functions at a late step in multivesicular body sorting. Mol. Biol. Cell *19*, 475–484.

Schmitt, A. P., Leser, G. P., Morita, E., Sundquist, W. I., and Lamb, R. A. (2005). Evidence for a new viral late-domain core sequence, FPIV, necessary for budding of a paramyxovirus. J. Virol. *79*, 2988–2997.

Scott, A., *et al*. (2005). Structural and mechanistic studies of VPS4 proteins. EMBO J. *24*, 3658–3669.

Strack, B., Calistri, A., Craig, S., Popova, E., and Gottlinger, H. G. (2003). AIP1/ALIX is a binding partner for HIV-1 p6 and EIAV p9 functioning in virus budding. Cell *114*, 689–699.

Stuchell-Brereton, M. D., Skalicky, J. J., Kieffer, C., Karren, M. A., Ghaffarian, S., and Sundquist, W. I. (2007). ESCRT-III recognition by VPS4 ATPases. Nature *449*, 740–744.

Takasu, H., Jee, J. G., Ohno, A., Goda, N., Fujiwara, K., Tochio, H., Shirakawa, M., and Hiroaki, H. (2005). Structural characterization of the MIT domain from human Vps4b. Biochem Biophys. Res. Commun. *334*, 460–465.

Tsang, H. T., Connell, J. W., Brown, S. E., Thompson, A., Reid, E., and Sanderson, C. M. (2006). A systematic analysis of human CHMP protein interactions: additional MIT domain-containing proteins bind to multiple components of the human ESCRT III complex. Genomics *88*, 333–346.

Van Damme, D., Inze, D., and Russinova, E. (2008). Vesicle trafficking during somatic cytokinesis. Plant Physiol. *147*, 1544–1552.

VerPlank, L., Bouamr, F., LaGrassa, T. J., Agresta, B., Kikonyogo, A., Leis, J., and Carter, C. A. (2001). Tsg101, a homologue of ubiquitin-conjugating (E2) enzymes, binds the L domain in HIV type 1 Pr55(Gag). Proc. Natl. Acad. Sci. USA *98*, 7724–7729.

von Schwedler, U. K., *et al*. (2003). The protein network of HIV budding. Cell *114*, 701–713.

Xiao, J., Xia, H., Zhou, J., Azmi, I. F., Davies, B. A., Katzmann, D. J., and Xu, Z. (2008). Structural basis of Vta1 function in the multivesicular body sorting pathway. Dev. Cell *14*, 37–49.

Zamborlini, A., Usami, Y., Radoshitzky, S. R., Popova, E., Palu, G., and Gottlinger, H. (2006). Release of autoinhibition converts ESCRT-III components into potent inhibitors of HIV-1 budding. Proc. Natl. Acad. Sci. USA *103*, 19140–19145.

Zhao, W. M., Seki, A., and Fang, G. (2006). Cep55, a microtubule-bundling protein, associates with centralspindlin to control the midbody integrity and cell abscission during cytokinesis. Mol. Biol. Cell *17*, 3881–3896.